MTOpen

Influence of Cationic Lipid Composition on Gene Silencing Properties of Lipid Nanoparticle Formulations of siRNA in Antigen-Presenting Cells

Genc Basha[1], Tatiana I Novobrantseva[2], Nicole Rosin[1], Yuen Yi C Tam[1], Ismail M Hafez[1], Matthew K Wong[3], Tsukasa Sugo[2], Vera M Ruda[4], June Qin[2], Boris Klebanov[2], Marco Ciufolini[5], Akin Akinc[2], Ying K Tam[6], Michael J Hope[6] and Pieter R Cullis[1]

[1]NanoMedicine Research Group, Department of Biochemistry and Molecular Biology Life Sciences Institute, University of British Columbia, Vancouver, British Columbia, Canada; [2]Alnylam Pharmaceuticals, Cambridge, Massachusetts, USA; [3]Centre for Drug Research and Development, University of British Columbia, Vancouver, British Columbia, Canada; [4]Cardiovascular Research Center and Center for Human Genetic Research, Massachusetts General Hospital and Harvard Medical School, Boston, Massachusetts, USA; [5]Department of Chemistry, University of British Columbia, Vancouver, British Columbia, Canada; [6]AlCana Technologies Inc., Vancouver, British Columbia, Canada

Lipid nanoparticles (LNPs) are currently the most effective *in vivo* delivery systems for silencing target genes in hepatocytes employing small interfering RNA. Antigen-presenting cells (APCs) are also potential targets for LNP siRNA. We examined the uptake, intracellular trafficking, and gene silencing potency in primary bone marrow macrophages (bmMΦ) and dendritic cells of siRNA formulated in LNPs containing four different ionizable cationic lipids namely DLinDAP, DLinDMA, DLinK-DMA, and DLinKC2-DMA. LNPs containing DLinKC2-DMA were the most potent formulations as determined by their ability to inhibit the production of *GAPDH* target protein. Also, LNPs containing DLinKC2-DMA were the most potent intracellular delivery agents as indicated by confocal studies of endosomal versus cytoplamic siRNA location using fluorescently labeled siRNA. DLinK-DMA and DLinKC2-DMA formulations exhibited improved gene silencing potencies relative to DLinDMA but were less toxic. *In vivo* results showed that LNP siRNA systems containing DLinKC2-DMA are effective agents for silencing *GAPDH* in APCs in the spleen and peritoneal cavity following systemic administration. Gene silencing in APCs was RNAi mediated and the use of larger LNPs resulted in substantially reduced hepatocyte silencing, while similar efficacy was maintained in APCs. These results are discussed with regard to the potential of LNP siRNA formulations to treat immunologically mediated diseases.

Received 2 February 2011; accepted 21 July 2011; published online 04 October 2011. doi:10.1038/mt.2011.190

INTRODUCTION

The therapeutic potential of siRNA-based drugs is considerable because they could allow selective gene silencing *in vivo* with high specificity and potency. However, effective delivery to targeted cells or tissues *in vivo* remains a major challenge.[1] Cationic lipid-nucleic acid complexes have advantages of low immunogenicity and ease of manufacture as compared to viral delivery systems;[2–4] however, they have limited use as systemic agents *in vivo* due to rapid clearance and toxicity issues. Well-defined lipid nanoparticle (LNP) systems containing encapsulated nucleic acid and utilizing ionizable cationic lipids to achieve long circulation lifetimes are more suited to *in vivo* applications.[5–7] Recent *in vivo* studies have demonstrated increasingly potent LNP delivery systems for silencing target genes in hepatocytes following systemic (intravenous, i.v.) injection,[8–13] resulting in systems with significant gene silencing at dose levels as low as 30 µg siRNA per kg body weight.

The major variable leading to increased potency of LNP siRNA delivery systems for gene silencing in hepatocytes has been improvements in the cationic lipid employed.[13] The cationic lipid is a critical component as a positively charged lipid is required to associate nucleic acid polymers with lipid-based delivery systems.[14–16] A positive charge on the carrier also promotes association with the negatively charged cell membrane to enhance cellular uptake.[17–19] In addition, it has been noted that cationic lipids combine with negatively charged lipids to induce nonbilayer structures that facilitate intracellular delivery.[20] Because charged LNPs are rapidly cleared from the circulation following i.v. injection,[21–23] work in our laboratory has focused on the development of ionizable cationic lipids with pKa values below 7.[6,7] Negatively charged polymers such as siRNA oligonucleotides can then be loaded into LNPs at low pH values (*e.g.*, pH 4) where the ionizable lipids display a positive charge. However, at physiological pH values, the LNPs exhibit a low surface charge compatible with longer circulation times. Recent work[13] has been focused on four species of ionizable cationic lipids, namely 1,2-dilineoyl-3-dimethylammonium-propane (DLinDAP), 1,2-dilinoleyloxy-3-*N*,*N*-dimethylaminopropane (DLinDMA), 1,2-dilinoleyloxy-keto-N,N-dimethyl-3-aminopropane (DLinK-DMA), and 1,2-dilinoleyl-4-(2-dimethylaminoethyl)-[1,3]-dioxolane (DLinKC2-DMA). It has been shown that LNP siRNA

Correspondence: *Genc Basha, Department of Biochemistry and Molecular Biology Life Sciences Institute, NanoMedicine Research Group, University of British Columbia, 2350 Health Sciences Mall, Vancouver, BC, V6T 1Z3, Canada. E-mail: gbasha@mail.ubc.ca*

systems containing these lipids exhibit remarkably different gene silencing properties in hepatocytes *in vivo*, with potencies varying according to the series DLinKC2-DMA>DLinK-DMA>DLinDMA>>DLinDAP employing a Factor VII gene silencing model.[13]

It is of obvious interest to extend these studies to extrahepatic targets. Cells of the immune system are attractive target tissues because LNP systems are preferentially accumulated by the fixed and free monocytes of the reticuloendothelial system following i.v. or subcutaneous (s.c.) administration.[24–27] Potential applications include treatment of inflammatory and autoimmune diseases that require silencing of genes in antigen-presenting cells (APCs).[28–31]

The objective of this study was to assess the gene silencing potency of LNP siRNA systems in primary APCs (pAPCs), namely macrophages (MΦ) and dendritic cells (DCs), using LNP-siRNA formulations containing DLinDAP, DLinDMA, DLinK-DMA, and DLinKC2-DMA. We demonstrate that LNP containing DLinKC2-DMA is most effective producing a significant siRNA-mediated *GAPDH* gene silencing *in vitro* in APCs at 1 μg/ml levels. Further, it is demonstrated that intravenous administration of LNP GAPDH-siRNA systems containing DLinKC2-DMA significantly inhibit the expression of *GAPDH* and CD45 protein *in vivo* in spleen and peritoneal MΦ and DCs. APC gene silencing is RNAi mediated as evidenced by 5′-RACE performed on peritoneal MΦ samples. In addition, it is demonstrated that by increasing LNP size, LNP can be effectively redirected to APCs from liver tissue.

RESULTS

LNP containing DLinKC2-DMA exhibits the most potent siRNA-mediated gene silencing *in vitro* in primary APCs

Primary bone marrow MΦ (bmMΦ) and bone marrow DCs (bmDCs) were isolated as indicated under Methods and incubated with 1 and 5 μg siRNA/ml scrambled or *GAPDH*-specific siRNA in LNP containing DLinDAP, DLinDMA, DLinKMA, and DLinKC2-DMA for 72 hours. Following treatment, *GAPDH* and control α-Tubulin expression was assessed using western blot analysis and flow cytometry. In bmMΦ treated with 1 μg/ml LNP siRNA, significant *GAPDH* silencing (>60%) was only observed for LNP containing DLinKC2-DMA. (**Figure 1a**). At dose levels of 5 μg/ml, LNPs containing DLinKC2-DMA were again the most potent gene silencing agents (80%). At this dose level, LNPs containing DLinDMA and DLinK-DMA also produced significant silencing (~60%), and DLinDAP was again ineffective.

Treatment of bmDCs with LNP-siRNA resulted in more pronounced *GAPDH* silencing than in bmMΦ (**Figure 1a**). At dose levels of 1 μg/ml, *GAPDH* protein was significantly reduced 72 hours after treatment with 1 μg/ml siRNA formulated in LNPs containing DLinDMA, DLinK-DMA, and DLinKC2-DMA, relative to the scramble control. The potency was further enhanced by increasing the siRNA dose to 5 μg/ml, where LNPs containing DLinKC2-DMA exhibited the highest silencing effects (83%). The gene silencing characteristics of LNP siRNA systems were also investigated following treatment of bone marrow APCs (bmAPCs) with 5 μg/ml siRNA for 72 hours where *GAPDH* protein expression was assessed by intracellular staining and analyzed by flow cytometry. In bmMΦ treated with siRNA encapsulated in LNPs containing DLinDMA, DLinK-DMA, or DLinKC2-DMA, the percentage of cells expressing *GAPDH* was decreased by 2.7-, 3.5-, and fourfold, respectively, relative to scramble controls (**Figure 1b**). Similar results were obtained following treatment of bmDCs where higher silencing potencies were observed (**Figure 1b**). Taken together, these data indicate that LNPs containing DLinKC2-DMA were the most efficient formulation for producing significant siRNA-mediated *GAPDH* gene knockdown *in vitro* at concentrations as low as 1 μg/ml.

LNPs containing DLinKC2-DMA exhibit highest uptake into APCs

It is important to determine why LNPs containing DLinKC2-DMA exhibit the most potent gene silencing characteristics. Two possibilities are that LNPs containing this lipid accumulate to higher levels in bmAPCs or that DLinKC2-DMA more effectively disrupts the endosomal membrane following uptake. As the fluorescence intensity of Cy3-labeled siRNA can be sensitive to breakdown by nucleases (P.J. Lin, unpublished results), the relative levels of uptake were measured by labeling LNPs with the lipid label SPDiO. Scrambled siRNA was encapsulated in SPDiO-labeled LNPs containing DLinDAP, DLinDMA, DLinK-DMA, and DLinKC2-DMA, and cellular uptake of siRNA and LNP lipid was monitored over 24 hours by measuring the fluorescence intensity of Cy3 and SPDiO in bmAPCs (**Figure 2b**). For all incubation times tested, significantly more uptake of siRNA and LNP lipid in LNPs containing DLinDMA, DLinK-DMA, and DLinKC2-DMA was observed relative to LNPs containing DLinDAP, suggesting that inefficient cellular uptake was at least partly responsible for the low levels of silencing seen with DLinDAP. Also, in bmMΦ and bmDCs, significantly more cellular uptake ($P = 0.014$ and $P = 0.011$, $P < 0.05$) of DLinKC2-DMA was detected, compared to DLinDMA and DLinK-DMA.

LNPs containing DLinKC2-DMA exhibit the greatest cytoplasmic delivery of siRNA as determined by fluorescence microscopy

To examine the fate of siRNA following uptake of LNP siRNA, a confocal microscopy study was undertaken to visualize the intracellular distribution of fluorescently labeled siRNA. Cy5-labeled siRNA was encapsulated in LNPs containing DLinDAP, DLinDMA, DLinK-DMA, and DLinKC2-DMA which were incubated with bmMΦ and bmDCs at 2 μg/ml siRNA for 2 hours. The cells were subsequently washed, and intracellular Cy5-labeled siRNA was followed for 1, 2, 4, and 8 hours (**Figure 3**). Similar levels of Cy5 fluorescence were observed in bmAPCs treated with DLinDAP, DLinDMA, DLinK-DMA, and DLinKC2-DMA at the 1-hour time point. However, after 8 hours, a lipid-dependent difference was observed in the intracellular distribution pattern of Cy5-siRNA in bmMΦ and bmDCs (**Figure 3a**). Fluorescently labeled siRNA delivered in LNPs containing DLinDAP exhibited a punctate pattern, characteristic of intracellular compartmentalization (**Figure 3a**). In contrast, siRNA delivered with DLinDMA LNPs showed a punctate pattern initially, and both a punctate and a diffuse distribution at later time points. siRNA delivered with DLinK-DMA and DLinKC2-DMA exhibited a predominantly

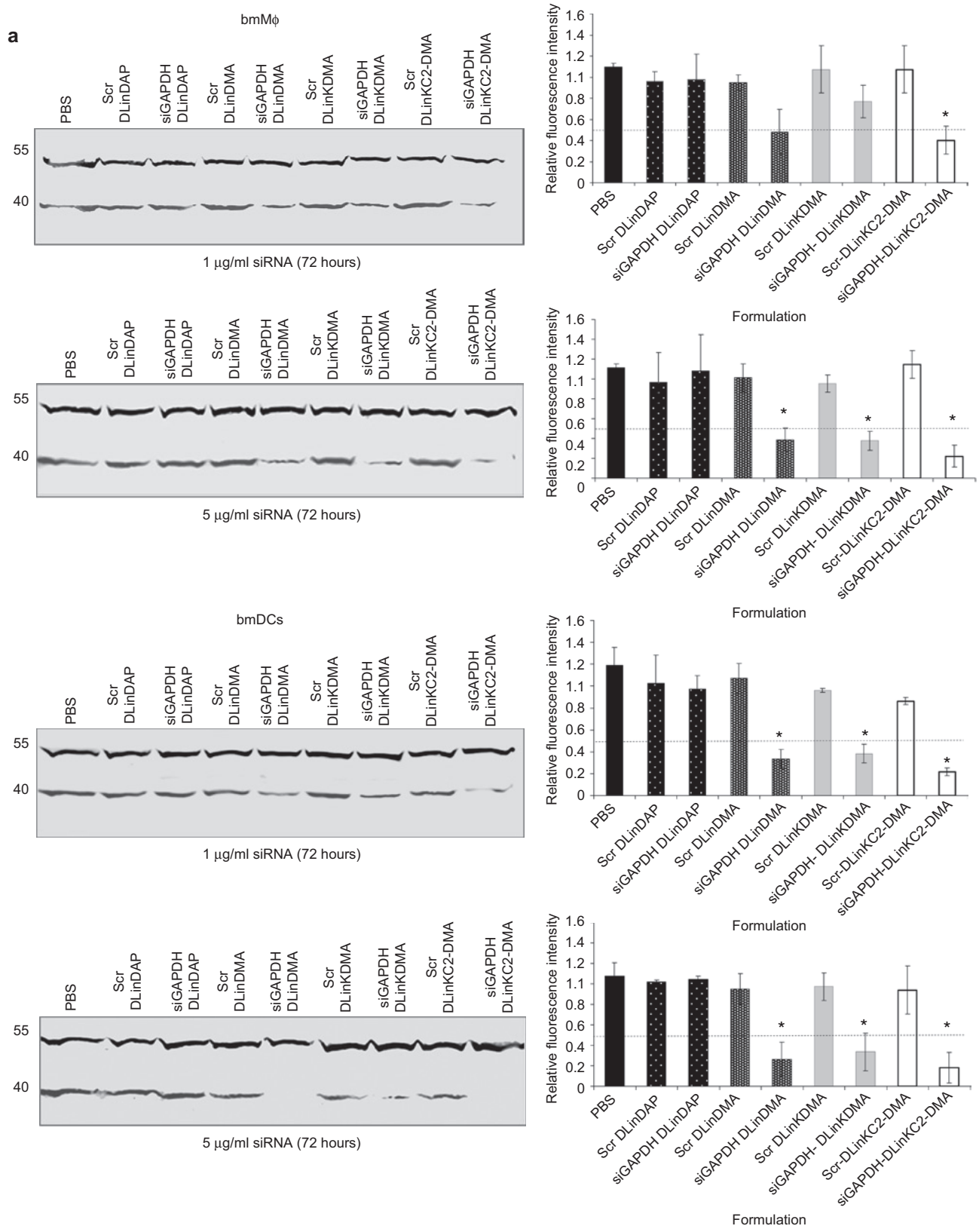

diffuse pattern even at early time points. The images of **Figure 3a** were quantified to assess the levels of siRNA-Cy5 fluorescence in the cytoplasm and in the punctate compartments following delivery with all LNPs tested (**Figure 3b,c**). This analysis revealed that both bmMΦ and bmDCs displayed mainly a punctate distribution of siRNA-Cy5 when treated with DLinDAP LNPs ($P = 0.017$, $P < 0.05$). LNPs containing DLinDMA, DLinK-DMA, and in particular DLinKC2-DMA delivered significantly more ($P = 0.016$,

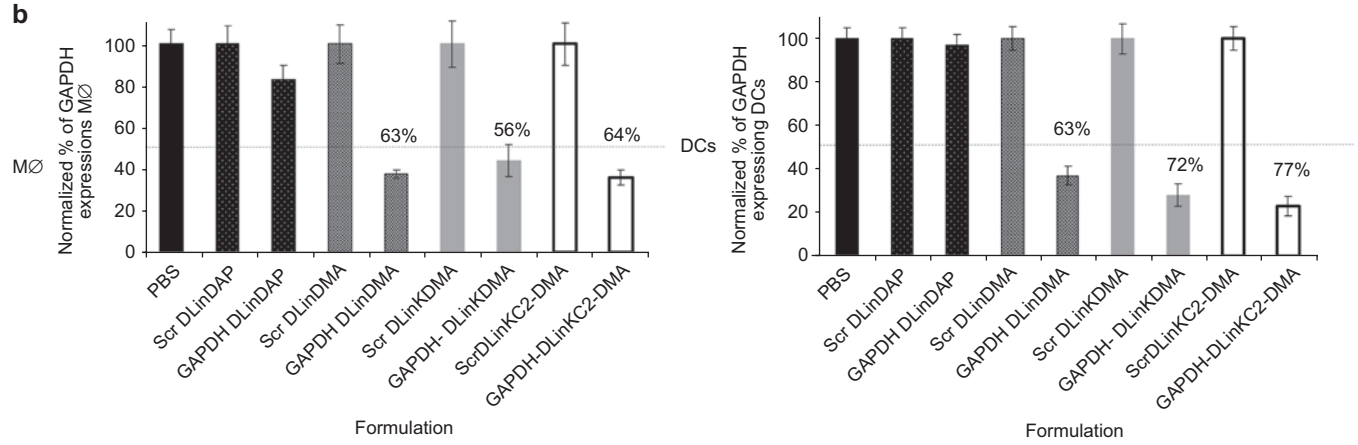

Figure 1 Effect of LNP composition on the siRNA-mediated silencing in APCs. (**a**) On day 8, bmMΦ and bmDCs were incubated with scrambled or anti-*GAPDH* siRNA encapsulated in LNPs at indicated doses, for 72 hours including PBS-treated control. Cells were lysed, and *GAPDH* and α-Tubulin expression was measured from protein extracts using SDS-polyacrylamide gel electrophoresis and western blotting following costaining with appropriate antibodies. The intensity and presence of the bands obtained were used to assess the efficacy and specificity of formulated siRNA. Blots are representative of three independent experiments. Data were quantified by assessing the relative intensity as calculated by dividing the absolute intensity of each sample band by the absolute intensity of the standard (loading control) and expressed as columns (mean ± SD, $n = 3$) shown beside each representative blot (* indicates $P < 0.05$). (**b**) The efficacy of LNP-siRNA was assessed following intracellular staining and analysis by flow cytometry. bmMΦ and bmDCs were treated with 5 µg/ml LNP-siRNA and after 72 hours, cells were fixed, permeabilized, and costained with anti-*GAPDH* and α-Tubulin followed by anti-rabbit IgG Alexa-647 and anti-mouse IgG-PE. Samples were acquired using a LSRII flow cytometer, and *GAPDH* and α-Tubulin protein expression was assessed. Data represent duplicates samples (mean ±) from two independent experiments. APC, antigen-presenting cells; bmDC, bone marrow dendritic cell; bmMΦ, bone marrow macrophages; LNP, lipid nanoparticles; PBS, phosphate-buffered saline.

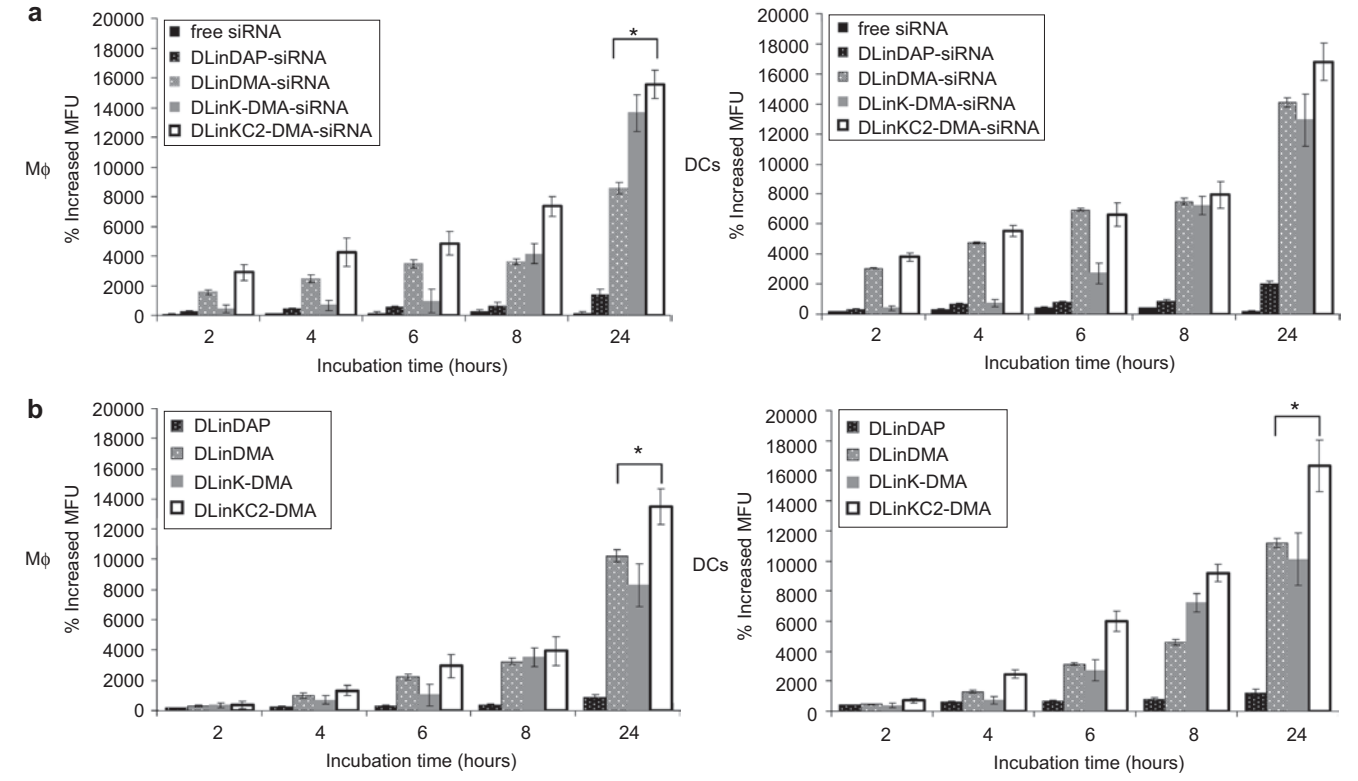

Figure 2 Intracellular presence of siRNA in bmMΦ and bmDCs is dependent on the LNP composition. (**a**) bmMΦ and DCs were incubated with 1 µg/ml LNP-siRNA labeled to Cy5 or (**b**) with 10 µg/ml scrambled containing SPDiO-labeled LNP for 2, 4, 6, 8, and 24 hours. Cells were harvested followed by intracellular siRNA-Cy5, and LNP-spDiO fluorescence was assessed by flow cytometry. The graphs depict percent increase (mean ± SD, $n = 3$) of mean fluorescence units (MFU) over time relative to untreated controls. Data are representative of three different experiments performed in triplicate (* indicates $P < 0.05$). bmDC, bone marrow dendritic cell; bmMΦ, bone marrow macrophages; LNP, lipid nanoparticles.

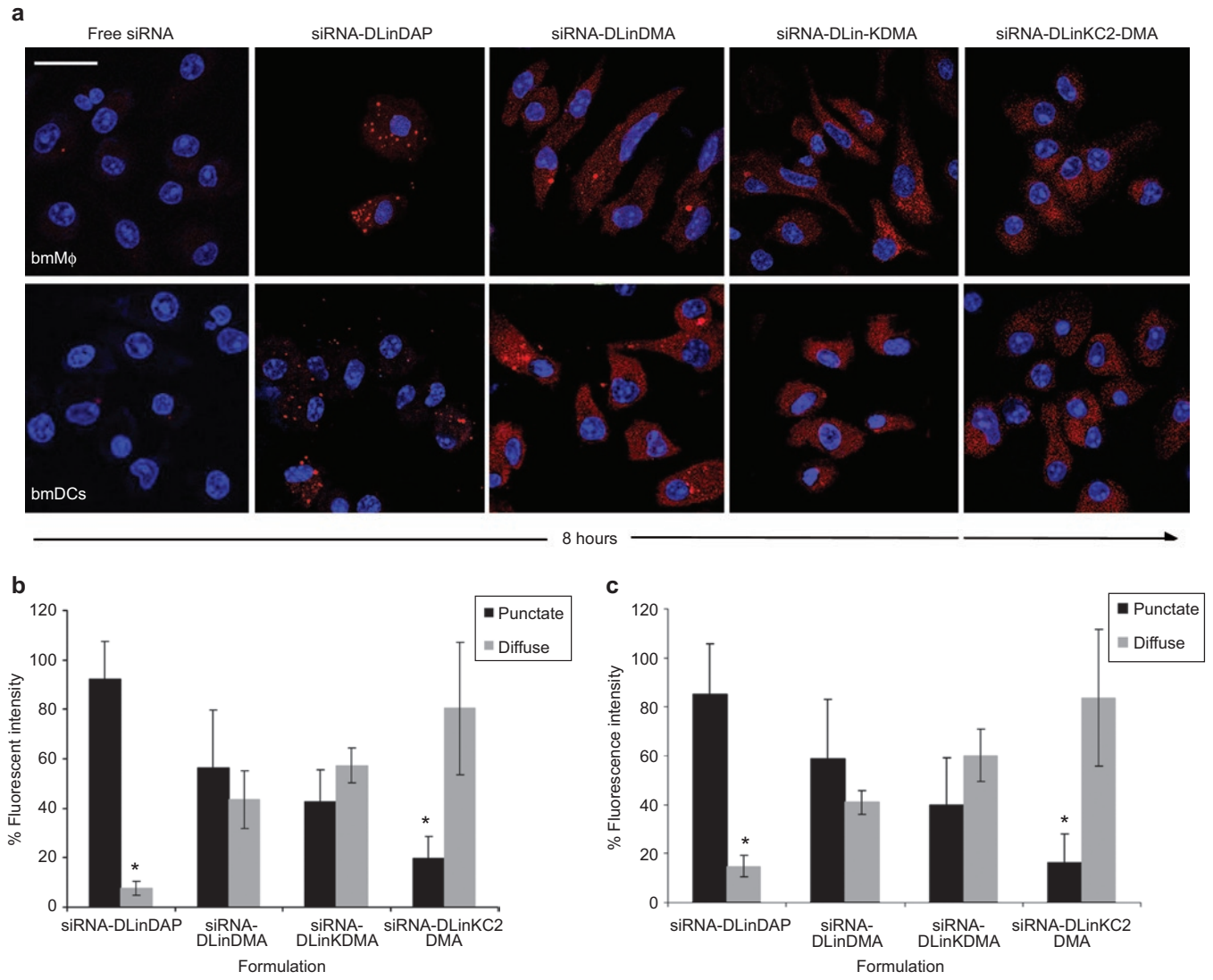

Figure 3 The intracellular pattern and distribution of siRNA are cationic lipid dependent. (**a**) bmMΦ and bmDCs were grown on glass coverslips, and siRNA-Cy5 encapsulated in indicated LNPs was added at 2 µg/ml for 2 hours. LNPs were washed off and siRNA distribution was visualized after 1, 2, 4, and 8 hours under an ICM with a ×60 objective. Data are representative of at least three images acquired and depict the intracellular distribution after 8-hour time point only. Bar = 5 µm. (**b**) Quantification of intracellular distribution of siRNA in bmMΦ and bmDCs. To examine the intracellular pattern of siRNA, "spots of interest" were drawn and fluorescence intensity was quantified as described in Materials and Methods. A minimum of three images were assessed for both (**b**) bmMΦ and (**c**) bmDCs. Graphs depict the mean value (±SD) expressed as average intensity units of ~30 cells obtained from multiple fields. Data are representative of two independent experiments (* indicates $P < 0.05$). bmMΦ, bone marrow macrophages; ICM, immunofluorescence confocal microscopy; LNP, lipid nanoparticles.

$P < 0.05$) siRNA to the cytosol (Figure 3b,c). Little or no Cy5-siRNA could be visualized intracellularly when cells were incubated with free siRNA at similar dose levels.

LNP siRNA systems deliver siRNA in APCs *via* endocytosis

To determine mechanisms of uptake and intracellular processing of LNP siRNA systems, primary bone marrow (BM)-derived MΦ and DCs were treated with 2 µg/ml LNP Cy5-siRNA for 2 hours, and internalized siRNA was chased for 0.5, 1, 2, 4, and 8 hours. Cells were stained with antibodies against early endosomes (EEA1) and examined under immunofluorescence confocal microscopy (ICM) to visualize the presence of siRNA in the endocytic pathway over time (Figure 4). As indicated by the yellow color of the vesicular compartments obtained by overlapping of siRNA (red) and endosomes (green), the LNP-siRNA systems enter the APCs primarily through the endocytic pathway. Colocalization of LNP-siRNA with endosomes was detected at early time points in both cell types (Figure 4). In agreement with the results of the previous section, the fluorescent pattern of siRNA delivered by DLinDAP LNPs remained punctate whereas for bmMΦ and bmDCs treated with DLinDMA, DLinK-DMA, and DLinKC2-DMA LNPs, cytoplasmic siRNA was observed after 2 hours of chase which increased after 4 hours of chase as indicated by the lack of colocalization of siRNA with EEA1 and increased cytosolic siRNA fluorescence (data not shown). Similar to earlier findings,

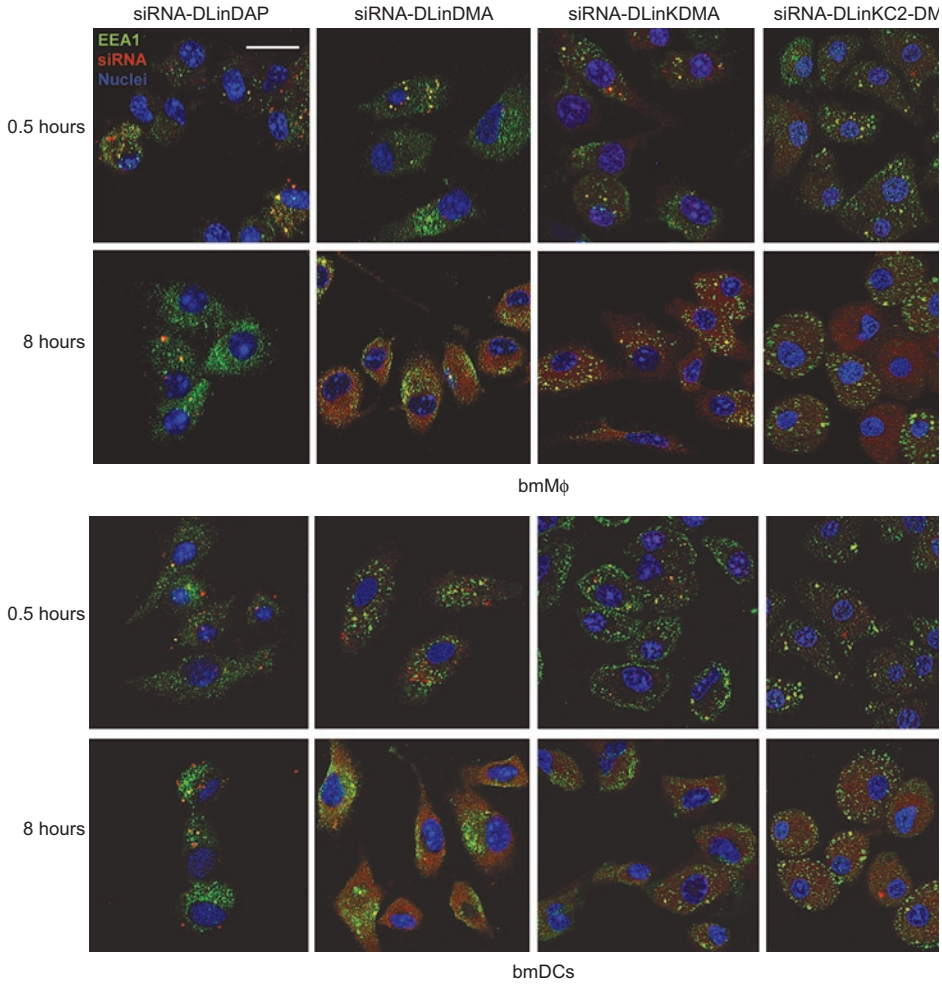

Figure 4 Influence of cationic lipid on endosomal escape of siRNA. Primary bmMΦ or bmDCs were treated with 2 µg/ml Cy5-siRNA encapsulated in LNPs as indicated, for 2 hours. LNP-siRNAs were washed off, and their localization was examined at 0.5, 1, 2, 4, and 8 hours under an ICM with a ×60 objective following staining with anti-EEA1 antibody to visualize the presence of siRNA (red) in early endosomes (green). Data are representative of three to five images acquired from two independent experiments. Only 0.5- and 8-hour time points are shown. bmDC, bone marrow dendritic cell; bmMΦ, bane marrow macrophages; ICM, immunofluorescence confocal microscopy; LNP, lipid nanoparticles. Bar = 5 µm.

DLinK-DMA and particularly DLinKC2-DMA LNPs delivered siRNA more effectively into the cytosol than DLinDMA LNPs. After 8 hours of chase, a complete separation of diffuse red siRNA and green endosomes was observed indicating relatively complete release of siRNA from the endosomes. In contrast, for LNP siRNA systems containing DLinDAP, the siRNA remained either in the endosomes or in other vesicular compartments as observed for both primary APCs.

To determine the eventual fate of LNP siRNA, primary APCs were treated with LNP-encapsulated siRNA for 2 hours followed by a 16-hour chase. Cells were then stained with EEA1 and LAMP1 antibodies to visualize early endosomes and lysosomes, respectively. Intracellular localization of siRNA was visualized, and the presence of siRNA in endosomes and lysosomes was quantified as described in Materials and Methods. The data demonstrate that siRNA delivered by DLinDAP LNPs remained in endosomes and lysosomes as indicated by colocalization (yellow color) of siRNA (red) with $EEA1^+$ endosomes (green), and lysosomes revealed by the overlapping (purple color) of siRNA (red) and LAMP1 (blue) (**Figure 5a**). In contrast, siRNA delivered with DLinDMA, DLinK-DMA, or DLinKC2-DMA showed typically a cytosolic distribution with only a small fraction detected in the endosomes or lysosomes (particularly in DCs) (**Figure 5a**). These results demonstrate that DLinDMA, DLinK-DMA, and in particular DLinKC2-DMA LNPs efficiently promote release of encapsulated siRNA into the cytosol following uptake *via* the endocytotic pathway.

LNPs containing DLinKC2-DMA are relatively nontoxic to APCs

In order to test the influence of the LNP formulations on the viability of primary APCs, bmAPCs were treated with various doses of LNP-siRNA or free siRNA and after 72-hour incubation, apoptosis and necrosis were assessed (**Supplementary Materials and Methods**). LNPs containing DLinDAP, DLinK-DMA, and DLinKC2-DMA displayed almost no toxicity in primary APCs (**Supplementary Figure S1**) even at the highest doses tested (5 µg/ml). LNPs containing DLinDMA, however, induced a significant

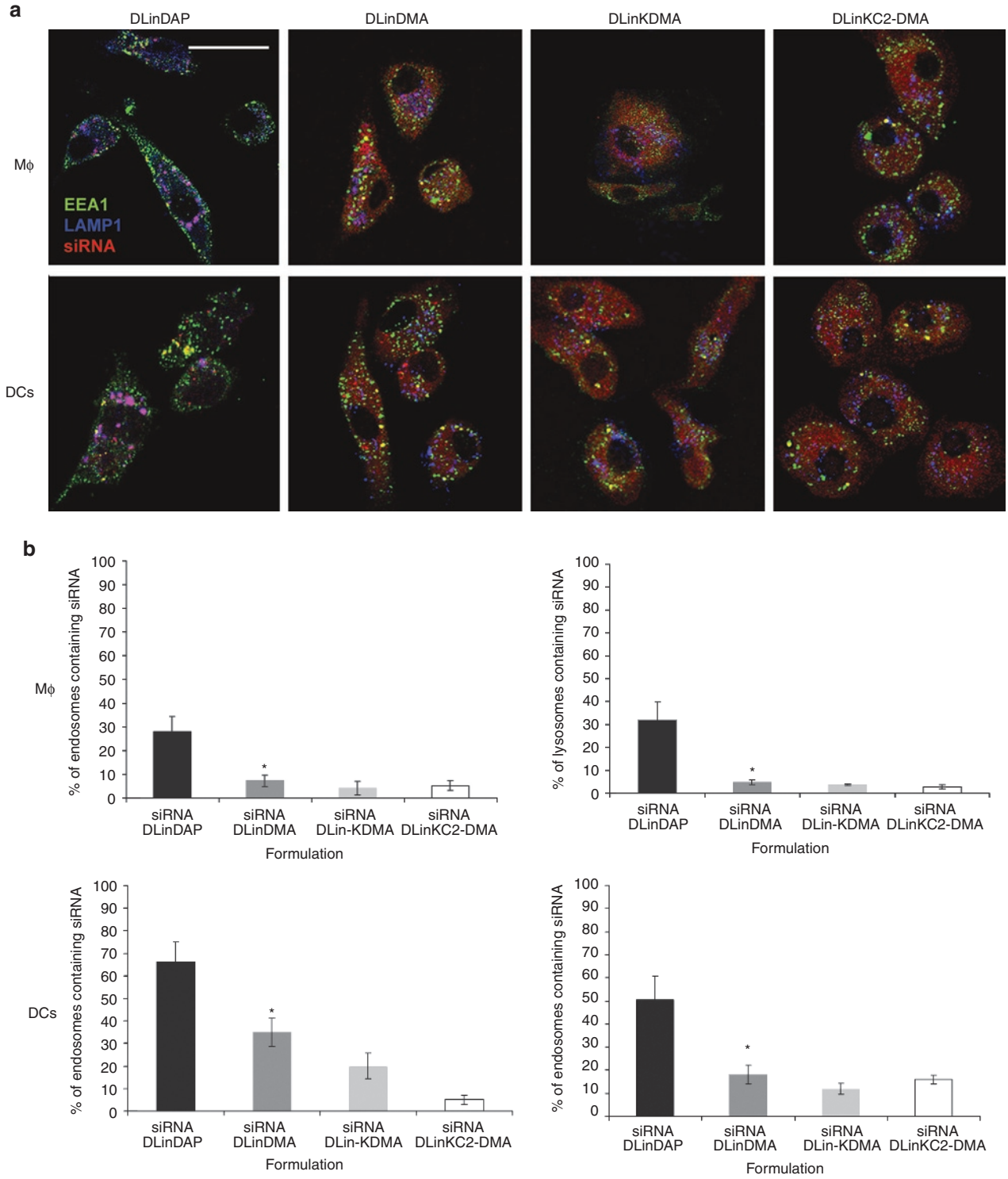

Figure 5 DlinDAP is inefficient in promoting endosomal release and cytoplasmic delivery in comparison with DLinDMA, DLinK-DMA, and DLinKC2-DMA. (**a**) bmMΦ and bmDCs were treated with 2 µg/ml Cy5-siRNA in LNPs for 2 hours, washed off and after 16-hour chase, cells were costained with anti-EEA1 (green) and anti-LAMP1 (blue) antibodies. Slides were viewed under an ICM to detect the presence of siRNA (red) in the endosomes or lysosomes. Data are representative of three to five images acquired from two independent experiments. Bar = 5 µm. (**b**) To quantify the presence of siRNA-Cy5 (red) in endosomes and lysosomes, absolute intensity of the overlapping color, yellow (green + red) or pink (blue + red), was expressed as percentage against absolute intensity of endosomes or lysosomes to evaluate the presence of siRNA in these organelles. Columns represent mean values (±SD) obtained from one of 20 Z-stacks of at least three microscopic fields viewed. Data are representative of two independent experiments (* indicates $P < 0.05$). bmDC, bone marrow dendritic cell; bmMΦ, bone marrow macrophages; ICM, immunofluorescence confocal microscopy; LNP, lipid nanoparticles.

increase in apoptotic cells even at doses as low as 1 μg/ml resulting in loss of cell viability (**Supplementary Figures S1** and **S2a**). Treatment with LNPs containing DLinK-DMA and DLinKC2-DMA resulted in the highest levels of intracellular siRNA at 72-hour post-treatment but exhibited little or no toxicity relative to DLinDMA-siRNA indicating that higher intracellular levels of siRNA did not result in increased toxicity. Overall, these data indicate that toxicity does not correlate with intracellular delivery and gene silencing potency and appears to be more directly associated with the particular cationic lipid employed.

Biodistribution of LNP-siRNA and intracellular delivery in tissue resident APCs

We set out to investigate the biodistribution of Cy3-labeled siRNA formulated with the LNPs under study, 30 minutes after systemic administration (**Supplementary Materials and Methods**). Confocal microscopy analysis revealed that fluorescence was measurable in all tissues analyzed (**Supplementary Figure S3a**). However, the overall distribution was organ and LNP dependent. It was observed that liver was the organ that took up significant amount of siRNA followed by spleen (data not shown), lymph nodes (LNs), and BM. Detectable levels of siRNA were observed in heart while insignificant amounts were revealed in the lungs. Also, a smaller amount of siRNA was observed following delivery with DLinDAP as assessed by lower fluorescent signal that was more evident in the liver. To further assess the siRNA delivery to tissue resident APCs and other cell types, such as T cells ($CD8^+$, $CD4^+$) and B cells that are abundant in the lymphoid organs, Cy5-siRNA was formulated with the best performing LNP and injected i.v. in mice. Flow cytometry analysis revealed that after 24 hours, Cy5-siRNA was measurable in liver, spleen, and LN APCs and less in the BM (**Supplementary Figure S3b**). In addition, very small amount of siRNA was measured in splenic $CD19^+$ B cells, and no delivery could be detected in spleen or LN $CD8^+$ and $CD4^+$ T cells (**Supplementary Figure S3c**). Taken together, these data indicate that siRNA LNPs are taken up by several organs and that our most efficient LNP DLinKC2-DMA is capable of delivering a substantial amount of siRNA in MΦ and DCs in lymphoid tissues. However, distribution is not necessarily equivalent to silencing, as siRNA needs to reach cytoplasm for activity.

LNPs containing DLinKC2-DMA can induce gene silencing in APCs *in vivo* following i.v. injection

The previous studies have shown that LNPs containing *GAPDH*-siRNA can induce gene silencing in primary APCs *in vitro* and that the most effective and least toxic formulations contain DLinKC2-DMA. It is of obvious interest to determine whether such formulations induce significant gene silencing *in vivo* following i.v. injection. Mice were dosed (5 mg/kg siRNA) with LNPs formulated employing DLinKC2-DMA and containing *GAPDH*-specific siRNA or control anti-FVII siRNA. APCs were harvested from peritoneal cavity and spleens 4 days later, and *GAPDH* expression was assessed in F4-80/CD11b- and CD11c-enriched cell populations using flow cytometry and western blotting. It was observed that treatment with LNP si*GAPDH* formulated with DLinKC2-DMA produced ~40% silencing by significantly reducing *GAPDH* production in peritoneal cavity MΦ and DCs ($P < 0.05$) and in the spleen-derived APCs as assessed by flow cytometry (**Figure 6a**). *GAPDH* silencing was also assessed by western blot analysis and revealed significant potency of DLinKC2-DMA as judged visually by the reduced *GAPDH* band in the APCs of each treated animal (**Figure 6b**). Quantification of the protein bands indicated that in spleen-derived APCs, *GAPDH* was reduced by 60% relative to siFVII control following systemic administration of DLinKC2-DMA-formulated si*GAPDH* whereas the expression levels of α-Tubulin were unchanged (**Figure 6c**). No substantial gene silencing was observed in LN APCs; in addition, siRNA delivery using the current systems failed to produce any silencing in B and T cells (data not shown). The discrepancy in gene silencing between spleen and LN APCs, however, could be partly explained by the overall difference in siRNA amount in these tissues determined by the blood supply and microenvironment. It could also be influenced by the heterogeneity of MΦ or DCs subsets. It is important to note that no treatment-related gross toxic effects were observed as determined by monitoring the weight loss (**Supplementary Figure S4**). These data demonstrate that LNPs containing DLinKC2-DMA are efficient promoters of siRNA-mediated gene silencing *in vivo* in spleen APCs.

Gene silencing in macrophages is RNAi mediated

To access whether the silencing observed in APCs was mediated by RNAi mechanism, cells of monocyte/macrophage lineage (CD11b positive) were purified from mice treated with *CD45* siRNA[11] encapsulated in the DLinKC2-DMA formulation; mRNA was isolated from these cells and subjected to rapid amplification of cDNA ends (5′-RACE), a method previously used to demonstrate that siRNA-mediated cleavage occurs.[12,32] 5′-RACE analysis revealed products of the expected sizes for *CD45* amplicon in samples treated with *CD45* specific but not with the control siRNA in the DLinKC2-DMA formulation (**Supplementary Figure S5**). Sequence analysis of cloned PCR products demonstrated that 46 of 48 products contained predicted cleavage at position (CTGGCTGAA/TTTCAGAGCA) for *CD45* siRNA in DLinKC2-DMA formulation. No specific cleavage sites were derived from the 5′-RACE samples treated with LNP encapsulated control siRNA (of 48 sequenced products). These results clearly demonstrate that the effect of siRNA in LNP treatment on *CD45* expression level observed is consistent with cleavage of the mRNA transcript *via* a targeted RNAi mechanism.

Designing siRNA LNP nanoparticles with differential activity in the liver and in APCs

As the standard DLinKC2-DMA-based LNPs were optimized for hepatic delivery of siRNA,[13] it mediates silencing of genes in hepatocytes with considerably better efficiency than in APCs. It was of interest to explore whether more APC-specific silencing could be achieved by redirecting particles away from the liver. To accomplish this, we exploited the fact that macrophages encounter and efficiently internalize particles of variable sizes (from 50 nm to 10 μm),[33] whereas efficient delivery to hepatocytes is likely restricted by the size of fenestrae in liver endothelium, estimated to be about 100–150 nm.[34] To compare liver and APC delivery in the same experiment, LNPs were formulated containing siRNAs targeting Factor VII (FVII), a liver-specific gene and *CD45*, a pan-leukocyte marker. Three formulations with an average size of 80 (normal), 240 (medium), and 360 nm (large) were tested

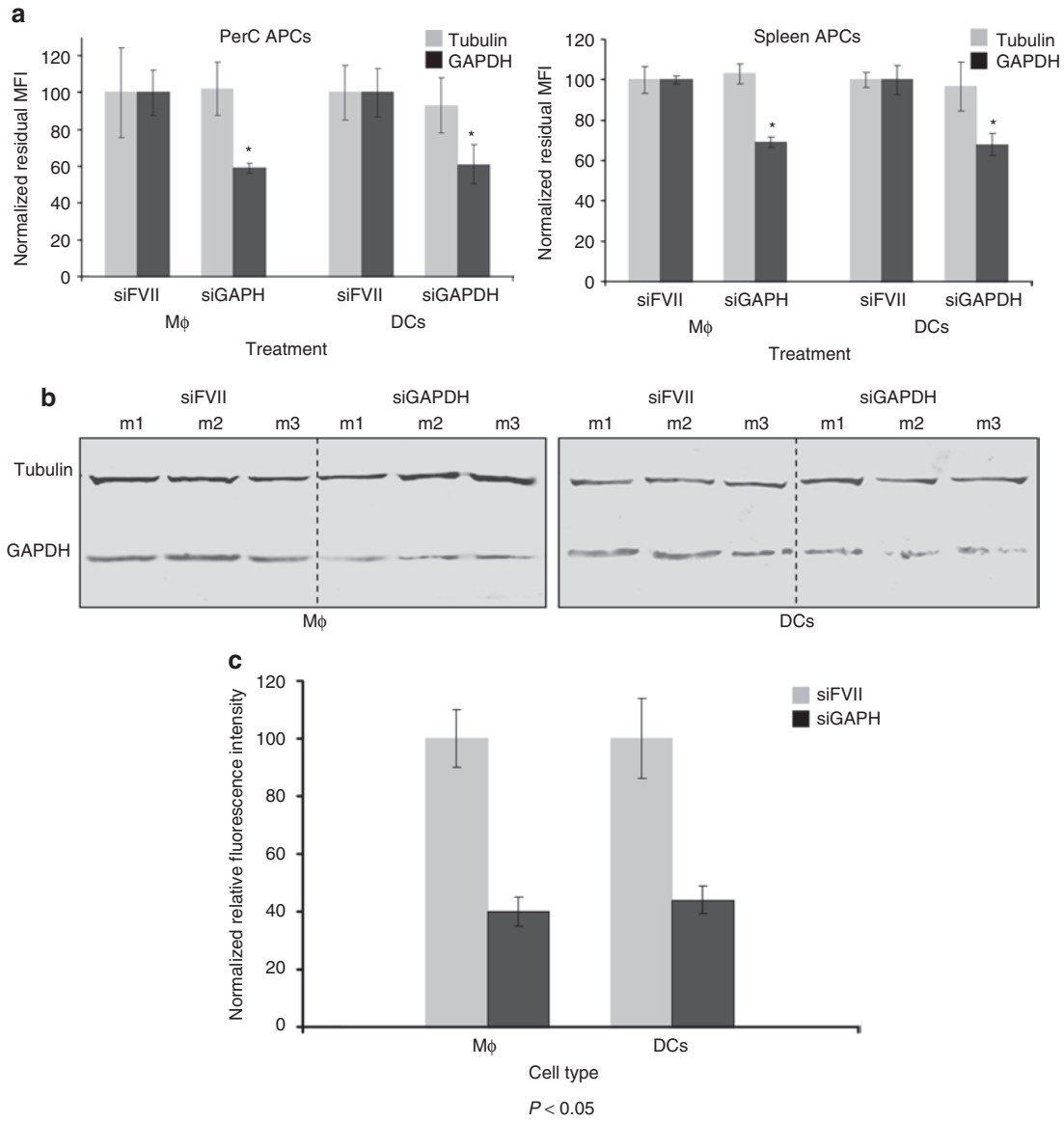

Figure 6 LNP siRNA systems containing DLinKC2-DMA can effectively silence target genes in APCs in vivo. Mice received 5 mg/kg si*GAPDH*, or siFVII as control formulated in DLinKC2-DMA LNPs by tail vein. Four days later, PerC APCs were obtained following peritoneal lavage, and spleen-derived APCs were isolated using magnetic beads. (**a**) PerC and spleen APCs were aliquoted and *GAPDH* and α-Tubulin protein expression was assessed by flow cytometry. Data represent mean (±SD) obtained from three independent mice. * $P < 0.05$. (**b**) Spleen APCs were lysed and protein expression was assessed using SDS-polyacrylamide gel electrophoresis and western blotting. (**c**) Data were quantified as described and normalized with the protein expression obtained following treatment with irrelevant siFVII considered 100%, to obtain the percent reduced *GAPDH* protein expressed as graphs (mean ± SD, $n = 3$). APC, antigen-presenting cell; LNP, lipid nanoparticles; PerC, peritoneal cavity.

with identical composition. These formulations contained either *CD45* siRNA or Luc/Factor VII (9:1) siRNA and were tested by i.v. bolus administration in naive C57BL/6 mice at 3 mg/kg ($n = 3$) (**Figure 7a**). A lower amount of Factor VII siRNA was used since the activity of the original formulation is about tenfold higher in hepatocytes relative to leukocytes; Luc siRNA was included in the Factor VII formulation to maintain the total dose of siRNA and LNPs constant for all experimental groups. Three days after injection, leukocytes were collected from the peritoneal cavity, and Factor VII was quantified from serum. Leukocytes were stained with antibodies for a combination of surface markers including *CD45*, F4-80, CD11b as a macrophage-specific marker. Silencing of *CD45* in macrophages is identical for these formulations (**Figure 7b**). However, reduction of serum FVII was decreased with increasing LNP size, consistent with decreased accessibility of larger LNPs through the liver fenestrae. Therefore, by utilizing larger LNPs, more APC-selective silencing may be achieved. We also set to investigate the duration of APC gene silencing *in vivo* using green fluorescent protein (GFP) transgenic mice. Data show that a marked suppression in GFP was observed in the peritoneal MΦ of siGFP-DLinKC2-DMA-treated mice 3 days following systemic administration (**Figure 7c**). Peritoneal cells were isolated at day 3 post-injection and seeded in a culture dish. Gene silencing persisted for ~14 days after initial dose.

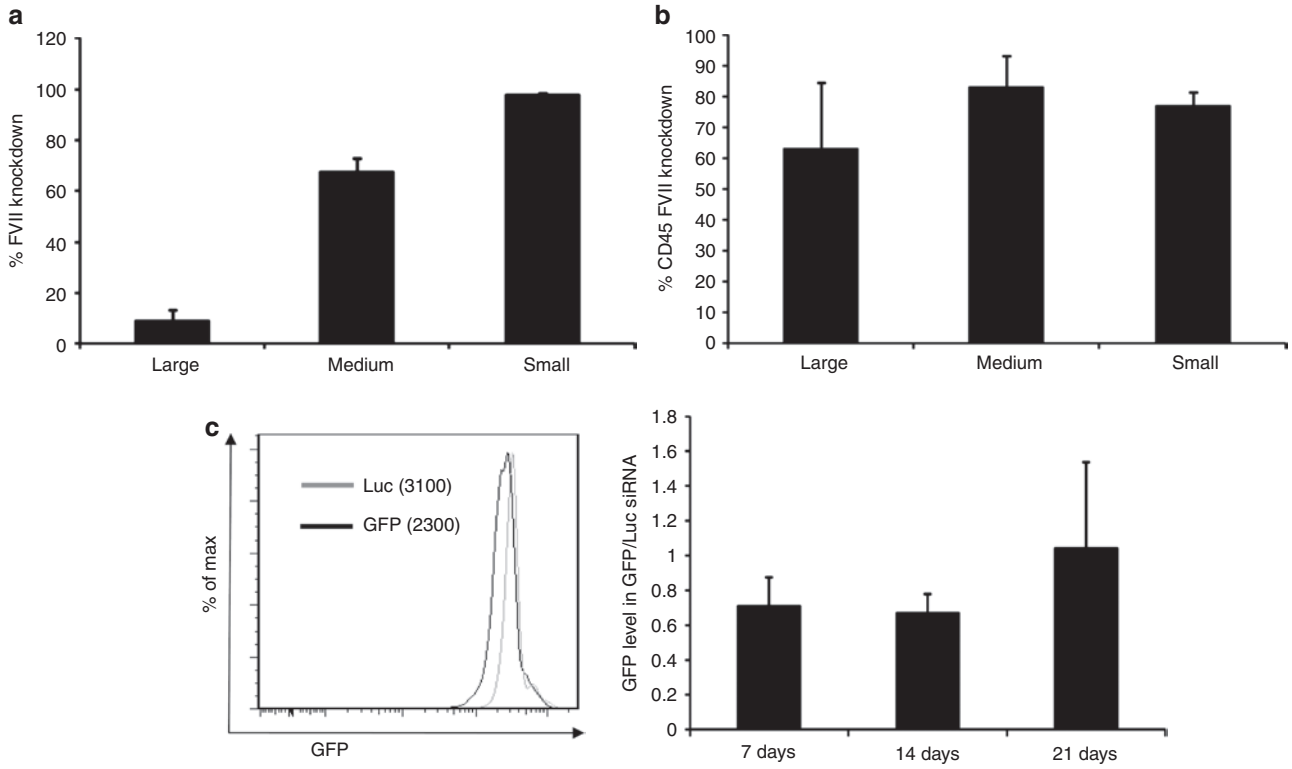

Figure 7 Large LNPs maintain potency in silencing gene expression in APC, but decrease activity in the liver. Mice in groups of three were injected with 3 mg/kg of total siRNA with either a mix of FVII and Luc siRNA or *CD45* siRNA. Serum and peritoneal cells were collected 72 hours after single bolus i.v. injection. Serum was analyzed for Factor VII level, peritoneal MΦ were identified, and CD45 was analyzed by flow cytometry. (**a**) Relative Factor VII level is plotted comparing animals injected with FVII+Luc and *CD45* (control) siRNA. (**b**) Graphs represent mean fluorescent intensity (MFI) (±SD, $n = 3$) values when comparing *CD45* siRNA to FVII+Luc (control) siRNA in DLinKC2-DMA LNPs. (**c**) Overlaid histograms represent fluorescent intrensities of GFP protein following treatment with siGFP or siLuc in DLinKC2-DMA. Graphs depict MFI (±SD, $n = 2$) at indicated time points. APC, antigen-presenting cell; GFP, green fluorescent protein; LNP, lipid nanoparticles.

Treatment with DLinKC2-DMA produces insignificant amount of TNF-α in *vitro* and *in vivo*

The potential of transfected MΦ to produce TNF-α in response to LNPs as a readout for cell stimulation by uptake was also studied. BmMΦ were incubated *in vitro* with different doses of siRNA formulated with the LNPs under study, or spleen MΦ of siRNA-DLinKC2-DMA-treated mice were isolated and TNF-α expression was assessed intracellularly by flow cytometry. Various expression levels of TNF-α were observed in bmMΦ following *in vitro* incubation with siRNA LNPs, and DLinDMA was the most potent cytokine inducer (**Figure 8a**). However, little amount of TNF-α was observed following DLinKC2-DMA treatment which showed levels similar to the least toxic LNP we know, the DLinDAP. Remarkably, MΦ transfected *in vivo* with DLinKC2-DMA expressed little amount of TNF-α (**Figure 8b**). Taken together the data indicate that there is a potential that LNP-siRNA complexes may induce cytokines in a dose-dependent manner and that the most efficient formulation DLinKC2-DMA produced insignificant amount of TNF-α in MΦ *in vivo*.

In vivo-transfected DCs maintain their function to activate T cells and migrate in lymph nodes

To test functional properties of LNP-treated APC, we tested the ability of *in vivo*-transfected DCs to activate T cells following antigen uptake (**Supplementary Materials and Methods**). For this, spleen DCs of mice injected with siRNA-DLinKC2-DMA were isolated, fed with ovalbumine, and their ability to activate the T-cell line B3Z[35] was assessed and compared with the untreated DCs. Flow cytometry analysis revealed that there was no difference between control and *in vivo*-transfected DCs in their ability to activate T cells following cross-presentation of ovalbumine antigen (**Supplementary Figure S6a**). Furthermore, the migration potential of *in vivo*-transfected GFP^+ DCs was also tested and compared with control DCs following injection in the foot pad of C57Bl6 mice. It was observed that almost equal number of cells migrated to inguinal LNs from the injection site in control and siRNA-DLinKC2-DMA-treated mice (**Supplementary Figure S6b**). Overall, the data indicate that there is essentially no functional impairment of DCs following their *in vivo* transfection with DLinKC2-DMA-formulated siRNA.

DISCUSSION

This work demonstrates that LNP siRNA systems containing appropriate ionizable cationic lipids can induce significant silencing of the "marker" target gene *GAPDH* for primary APCs both *in vitro* and *in vivo*. There are three aspects of these results that warrant further discussion, including the reasons why LNPs containing DLinKC2-DMA exhibit superior gene silencing potencies *in vitro* for APCs, the significance of the observation that LNP siRNA systems containing DLinKC2-DMA are effective gene

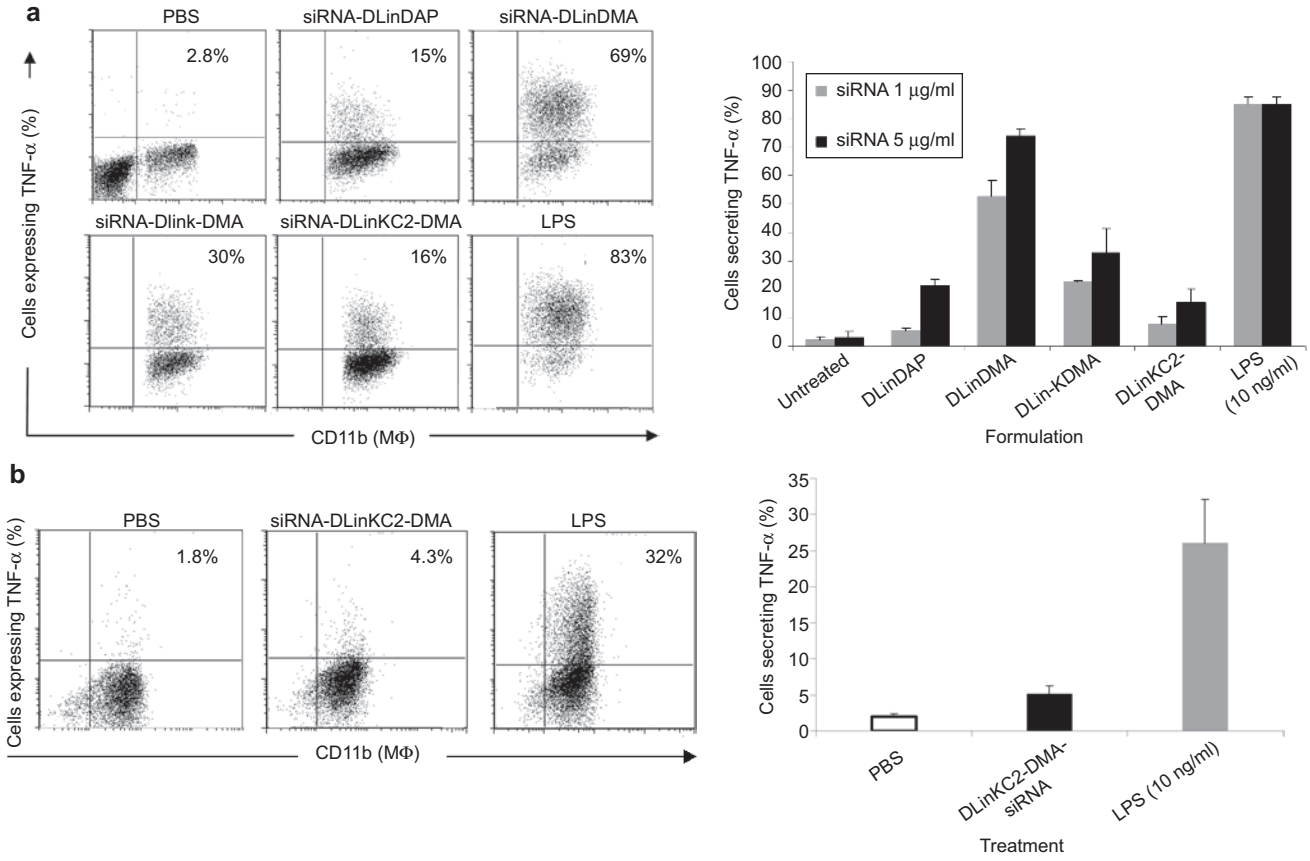

Figure 8 DLinKC2-DMA produces small amount of TNF-α in vitro and in vivo. BmMΦ were treated with 1 and 5 μg/ml siRNA encapsulated in all LNPs under study including PBS or LPS 10 ng/ml. Cells were costained with CD11b-FITC and anti-TNF-α PE antibody to assess the presence of TNF-α intracellularly using flow cytometry. (**a**) Representative dot plots indicating the presence of TNF-α intracellularly following treatment with LNPs are shown. Graphs represent normalized TNF-α expression in bmMΦ (±SD, $n = 3$). (**b**) Spleen MΦ were isolated from PBS or DLinKC2-DMA-siRNA-treated mice, and TNF-α was detected in MΦ using flow cytometry. Representative dot plots indicating the expression of TNF-α are shown. Graphs depict normalized TNF-α expression in spleen MΦ (±SD, $n = 3$). BmMΦ, bone marrow macrophages; LNP, lipid nanoparticles; LPS, lipopolysaccharide; PBS, phosphate-buffered saline.

silencing agents for MΦ and DCs *in vivo* together with potential ways in which the activity could be improved and finally the potential applications of LNP siRNA systems that are able to silence genes in immune cells.

The results presented indicate that LNP siRNA systems containing DLinKC2-DMA are the most potent formulations for achieving silencing of *GAPDH* in MΦ and DCs *in vitro*. These results are similar to behavior noted for LNP siRNA systems for FVII gene silencing *in vivo*[13] where it was observed that the potency varied according to DLinKC2-DMA> DLinK-DMA>DLinDMA>DLinDAP following i.v. injection. The *in vitro* results presented here indicate similar activities, with the exception that LNPs containing DLinDMA were somewhat more effective than LNPs containing DLinK-DMA for *GAPDH* silencing (**Figure 1**). The relative ineffectiveness of the DLinDAP formulations could be partly related to rapid hydrolysis in the endosome of the labile ester linkages present in this cationic lipid (P.J. Lin, unpublished results). Hydrolysis of DLinDAP will reduce disruption of the endosomal membrane, therefore siRNA release into the cytoplasm, as well as expose encapsulated siRNA to potential degradation by endogenous nucleases in the endosome.[36] However, it is also clear that the levels of uptake of the DLinDAP-containing systems are much lower than for LNPs containing other cationic lipids (**Figure 2**). Further, it is also obvious that after accumulation, LNPs containing DLinDAP are much less effective agents for facilitating endosomal escape of encapsulated siRNA as evidenced by the very low diffuse-to-punctate ratio for accumulated siRNA for these systems (**Figure 3**). LNPs containing DLinKC2-DMA are accumulated at higher levels than LNPs containing DLinDMA or DLinK-DMA for both MΦ and DCs (**Figure 2**) which likely accounts for the higher gene silencing activity noted for these formulations. Similarly, LNPs containing DLinDMA and DLinKC2-DMA are accumulated to approximately similar levels and exhibit about the same levels of silencing potency. It is interesting to note, however, that the siRNA intracytoplasmic delivery capability of LNPs containing DLinKC2-DMA is considerably improved over those containing DLinDMA as indicated by the low punctate-to-diffuse ratio observed for the DLinKC2-DMA system (**Figure 3**), which would also be expected to enhance silencing potency.

The second area of discussion concerns the significance of the observation that LNP siRNA systems containing DLinKC2-DMA can silence genes in spleen and peritoneal cavity MΦ and DCs as well as ways in which the transfection potency of the LNP systems employed here could be improved. There have been a variety of

reports demonstrating gene silencing in APCs following i.v. administration of siRNA in free or encapsulated form. Free siRNA can result in silencing of liver MΦ following hydrodynamic (high volume) tail vein (HTV) injection of siRNA.[37–39] However, aside from providing proof of concept on the effectiveness of siRNA *in vivo* to inhibit endogenous genes, there are drawbacks to this method that make its application in clinical practice unlikely. In addition to a transient toxicity, the use of HTV injection results in delivery of siRNA primarily to the liver. A variety of nanoparticle delivery approaches have been described such as targeting of siRNA to MΦ[40] using glucan-encapsulated siRNA particles (GeRPs), integrin-targeted stabilized nanoparticles (I-tsNPs) for leukocytes[41], and immunoliposomes for DCs.[42] However, all these methods have limitations. For example, despite the advantage of ease of oral administration for the GeRPs, APC transfection is relatively inefficient. Similarly, the finding that following systemic administration, I-tsNPs were preferentially accumulated in the gut, suggests primarily tissue-specific indications. Zheng and colleagues[42] have employed imunoliposomes conjugated to DC-specific antibody for targeting CD40 on DCs. A possible disadvantage of this approach for clinical applications is that chimeric antibodies as targeting agents have been reported to elicit immune responses and could contribute to unpredictable side effects.[43,44] The LNP system employed here exhibits a number of advantages over previous methods, including high siRNA encapsulation efficiencies (>95%), relatively low toxicity *in vitro* and *in vivo* as indicated by parameters such as weight loss, no impairment of DC antigen presentation and migration, as well as minute induction of cytokines, particularly for the best performing LNP, in addition to the ability to silence APCs in anatomically distant locations such as peritoneal cavity and spleen.

It is likely that improvements to the LNP siRNA systems outlined here will be possible. By way of comparison, similar LNP siRNA systems have recently been demonstrated to achieve gene silencing in hepatocytes following i.v. administration at dose levels as low as 30 μg siRNA/kg body weight.[13] The improved potency of these systems as compared to the dose levels of 5 mg siRNA/kg body weight employed here stems from at least two factors. First, Semple and colleagues[13] employed higher levels of cationic lipid and lower levels of PEG-lipids and it is expected that significantly improved potency will be observed for silencing genes in APCs when such formulations are employed. Second, it has also been demonstrated that LNP-induced gene silencing in hepatocytes benefits from stimulated uptake due to association of ApoE with the LNP particles following i.v. injection.[45] It is likely that the inclusion of ligands that stimulate uptake into APCs will bring similar benefits to gene silencing in immune cells. Alternatively, the strategy of increasing LNP size can also improve APC-specific silencing as demonstrated here.

There are many potential applications for LNP siRNA systems that can silence genes in APC and we only point out three of them here. First, inactivation of *CD45* correlates with long-term engraftment of allogeneic and xenogeneic heart and kidney transplants,[46] whereas in patients with Alzheimer's disease *CD45* expression is upregulated on microglia cells.[47] Thus, targeting *CD45* in MΦ using LNP-siRNA has direct applicability to clinical transplantation, treatment of autoimmune diseases or neuroinflammation associated with Alzheimer's disease.[48] Second, silencing CD40 in DCs could be an effective method for minimizing autoimmune responses by inducing antigen-specific immune suppression.[42] Finally, RNAi techniques may be useful to improve cancer immunotherapies. Immune activation in the tumor microenviroinment combined with siRNA that targets immune suppressor genes in tumor-infiltrating APCs represents a potentially effective approach for cancer immunotherapy.[49]

MATERIALS AND METHODS

Preparation of LNPs and siRNA encapsulation. The cationic lipids 1,2-dilineoyl-3-dimethylammonium-propane (DLinDAP), 1,2-dilinoleyloxy-3-*N*,*N*-dimethylaminopropane (DLinDMA), 1,2-dilinoleyloxy-keto-N,N-dimethyl-3-aminopropane (DLinK-DMA), 1,2-dilinoleyl-4-(2-dimethylaminoethyl)-[1,3]-dioxolane (DLinKC2-DMA), (3-o-[2″-(methoxypolyethyleneglycol 2000) succinoyl]-1,2-dimyristoyl-sn-glycol (PEG-S-DMG), and R-3-[(ω-methoxy-poly(ethylene glycol)2000) carbamoyl]-1,2-dimyristyloxlpropyl-3-amine (PEG-C-DOMG) were provided by Tekmira Pharmaceuticals (Vancouver, Canada) or synthesized as described elsewhere.[13] Cholesterol was purchased from Sigma (St Louis, MO). The anti-Factor VII Cy5-labeled siRNA was provided by Alnylam Pharmaceuticals (Cambridge, MA) and was used in a free form or was encapsulated in LNPs containing DLinDAP, DLinDMA, DLinK-DMA, and DLinKC2-DMA (cationic lipid:DSPC:CHOL: PEG-S-DMG or PEG-C-DOMG at 40:10:40:10 molar ratios). When required, 0.2% SP-DiOC18 (Invitrogen, Burlington, Canada) was incorporated to assess cellular uptake, intracellular delivery, and biodistribution. For gene silencing experiments, anti-*GAPDH* siRNA (si*GAPDH*) was purchased from Dharmacon. The preformed vesicle method of siRNA encapsulation was employed as described elsewhere.[6–7,13] Briefly, the lipid mixtures comprised of cationic lipid:DSPC:cholesterol:PEG-c-DOMG (40:10:40:10 molar ratio) were dissolved in ethanol to a final lipid concentration of 10 mmol/l. This ethanol solution of lipid was added drop-wise to 50 mmol/l citrate, pH 4.0 to form multilamellar vesicles to produce a final concentration of 30% ethanol vol/vol. Large unilamellar vesicles were formed following extrusion of multilamellar vesicles through two stacked 80 nm Nuclepore polycarbonate filters using the Extruder (Northern Lipids, Vancouver, Canada). Encapsulation was achieved by adding siRNA dissolved at 2 mg/ml in 50 mmol/l citrate, pH 4.0 containing 30% ethanol vol/vol drop-wise to extruded preformed large unilamellar vesicles and incubation at 31 °C for 30 minutes with constant mixing to a final siRNA/lipid weight ratio of 0.06/1 wt/wt. Removal of ethanol and neutralization of formulation buffer were performed by dialysis against phosphate-buffered saline (PBS), pH 7.4 for 16 hours using Spectra/Por 2 regenerated cellulose dialysis membranes. Nanoparticle size distribution was determined by dynamic light scattering using a NICOMP 370 particle sizer, the vesicle/intensity modes, and Gaussian fitting (Nicomp Particle Sizing, Santa Barbara, CA). The particle size for all three LNP systems was ~70 nm in diameter. siRNA encapsulation efficiency was determined by removal of free siRNA using VivaPureD MiniH columns (Sartorius Stedim Biotech) from samples collected before and after dialysis. The encapsulated siRNA was then extracted from the eluted nanoparticles and quantified at 260 nm. siRNA to lipid ratio was determined by measurement of cholesterol content in vesicles using the Cholesterol E enzymatic assay from Wako Chemicals USA (Richmond, VA).

Preparation of large LNPs. A lipid premix solution (20.4 mg/ml total lipid concentration) was prepared in ethanol containing DLinKC2-DMA, DSPC, and cholesterol at 50:10:38.5 molar ratios. Sodium acetate was then added to the lipid premix at a molar ratio of 0.75:1 (sodium acetate:DLinKC2-DMA). The lipids were subsequently hydrated by combining the mixture with 1.85 volumes of citrate buffer (10 mmol/l, pH 3.0) with vigorous stirring, resulting in spontaneous liposome formation in aqueous buffer containing 35% ethanol. The liposome solution was then incubated at 37 °C to

allow for time-dependent increase in particle size. Aliquots were removed at various times during incubation to investigate changes in liposome size by dynamic light scattering (Zetasizer Nano ZS, Malvern Instruments, Worcestershire, UK). Once the desired particle size was achieved, an aqueous PEG lipid solution (stock = 10 mg/ml PEG-DMG in 35% (vol/vol) ethanol) was added to the liposome mixture to yield a final PEG molar concentration of 3.5% of total lipid. Upon addition of PEG-lipids, the liposomes maintained their size, effectively quenching further growth. siRNA was then added to the empty liposomes at an siRNA to total lipid ratio of approximately 1:10 (wt:wt), followed by incubation for 30 minutes at 37 °C to form loaded LNPs. The mixture was subsequently dialyzed overnight in PBS and filtered with a 0.45-μm syringe filter.

Cell culture of primary APCs. bmAPCs were prepared from BM progenitors by flushing 6- to 8-week-old C57BL/6 (Jackson Laboratory) mouse femurs and tibias with PBS. After 2 washes, BM-derived progenitor cells were cultured in 6-well plates at 2×10^6 cells/ml in 5 ml in complete medium (RPMI 1640 supplemented with 2 mmol/l L-glutamine, 100 U/ml penicillin, 100 μg streptomycin, 10% fetal calf serum, sodium pyruvate (1 mmol/l), nonessential aminoacids (1 mmol/l), and Hepes (10 mmol/l) all from Invitrogen supplemented with either 10% 1x L929 cell conditioned media for differentiation of MΦ or X63-Ag8-plasmacytoma-derived GM-CSF (gift from David Gray, University of Edinburgh, Edinburgh, UK) 80 μl/5 ml for DCs. On day 8, bmMΦ were stained with antibodies against I-Ab (AF6.120.1) and CD11b whereas bmDCs were stained with H-2Kb (AF6.88), I-Ab, CD11c (HL3) (Pharmingen), and DEC-205 to assess their purity and stage of maturation. All cells were cultured in a humidified atmosphere of 5% CO_2 at 37 °C. After 8 days of culture, more then 80% of cells expressed MΦ- and DC-specific markers, respectively, as determined by flow cytometry.

***Silencing of APCs* in vitro.** The day prior to treatment, bmMΦ and bmDCs were washed and replenished with fresh media in the original plates. SiRNA against *GAPDH* (sense sequence: UGGCCAAGGUCAUCCAUGA) or negative control scrambled siRNA encapsulated in DLinDAP, DLinDMA, DLinK-DMA, and DLinKC2-DMA LNPs was added on day 8 of culture at 1 and 5 μg/ml final concentration and incubated for 72 hours at 37 °C and 5% CO_2. In each experiment, one well was treated PBS and served as a negative control. The media was changed every other day while the concentration of siRNA was maintained at required concentrations. Following treatment, *GAPDH* and α-Tubulin protein expression was measured to assess the efficacy and specificity of formulated siRNA.

Western blotting: Adherent bmMΦ were washed with cold PBS in the original plate followed by addition of RIPA lysis buffer containing 1% Nonidet P-40 (NP-40), 120 mmol/l NaCl, 4 mmol/l $MgCl_2$, 20 mmol/l Tris-HCl pH 7.6, protease inhibitor cocktail (Roche) 1 mmol/l PMSF and NaF, and incubated for 45 minutes at 4 °C. Cells were harvested by scraping the adherent cells with a cell-scraper. Cell lysates were then transferred in to a microcentrifuge tube and spun at maximum speed for 10 minutes. Floating bmDCs were washed 1 x with cold PBS and lysed by resuspending and incubating in RIPA lysis buffer for 45 minutes. The lysates were spun for 10 minutes at maximum speed at 4 °C, and protein concentration was assessed using Bradford assay (Biorad). About 5 μg protein sample was resuspended in appropriate volume of 10% SDS-containing Laemmli buffer and boiled for 5 minutes at 100 °C. Samples were subsequently analyzed on a 10% gradient SDS-polyacrylamide gel electrophoresis (PAGE). The gel was transferred onto a nitrocellulose membrane (PallCorporation, Pensacola, FL), blocked with Odyssey Blocking Buffer (Li-cor Biosciences, Lincoln, NE) and costained with rabbit anti-*GAPDH* and mouse anti α-Tubulin antibodies (Santa Cruz Biotechnology, Santa Cruz, CA) at 1:200 dilution overnight. IRDye 680CW donkey anti-rabbit IgG (H+L) and IRDye 800CW donkey anti-mouse IgG (H+L) (Li-Cor Biosciences) were used at 1:2000 dilution to detect the *GAPDH* and α-Tubulin, respectively, following 2-hour incubation in the dark. Blots were scanned on an Odyssey Infrared Imaging System to visualize the bands of interest. Images were acquired at medium intensity and resolution 3. Quantification of the data was performed using Photoshop 9.0 CS2 software. Absolute intensity for each selected sample band was obtained by multiplying the pixel value with the average intensity. The relative intensity was then calculated by dividing the absolute intensity of each sample band by the absolute intensity (pixel value × average intensity) of the standard (loading control).

Flow cytometry: The efficacy of formulated siRNA was also determined by intracellular staining and assessment with flow cytometry. For this, 72 hours following treatment with 5 μg/ml si*GAPDH* or scramble control formulated with the LNPs under study, bmMΦ and bmDCs were harvested, transferred into microcentrifuge tubes and spun at 12,000 for 4 minutes. Cells were washed twice with FACS staining buffer (2% FBS, 1 mmol/l EDTA, and 0.1% Na Azide) and resuspended in fixation buffer (paraformaldehyde 4%) for 20 minutes. Next, they were resuspended in permeabilization buffer (saponin 0.5%, Sigma Aldrich, St. Louis, MO), aliquoted, and costained with rabbit anti-*GAPDH* and mouse anti α-Tubulin antibodies at 1:20 dilution for 30 minutes at room temperature. After two washings with permeabilization buffer, cells were labeled with goat anti-rabbit IgG (H+L) Alexa-647 (Invitrogen) and goat anti-mouse IgG (H+L) PE-conjugated antibodies in the dark, to detect the *GAPDH* and α-Tubulin, respectively, in bmAPCs. Unstained and cells incubated with isotype controls were included in all experiments. Next, bmAPCs were washed extensively with permeabilization buffer and PBS, followed by resuspension in 300 μl FACS staining buffer prior to data acquisition. The LSRII flow cytometer (BD Biosciences, San Jose, CA) and FACSDiva software were used to measure protein expression following acquisition of 10,000 events. Data were analyzed by FlowJo software. *GAPDH* expression values were normalized against α-Tubulin and expressed as percent reduced fluorescence relative to scramble control that was considered 100%.

Intracellular delivery of siRNA by LNPs. On day 8, bmMΦ and bmDCs were transferred to 24-well plates, treated with 1 μg/ml siRNA-Cy5 in a free form or encapsulated in DLinDAP, DLinDMA, DLinK-DMA, and DLinKC2-DMA LNPs, and maintained at 37 °C. Incubation was stopped by washing off the media and harvesting the cells after 2, 4, 6, 8, and 24 hours. Cells were also incubated with 0.5, 1, or 5 μg/ml Cy5-labeled siRNA for 24 hours to assess the dose-dependent intracellular delivery of siRNA. To investigate whether the intracellular bioavailability of siRNA in bmAPCs correlates with the cellular uptake of LNPs, in parallel scrambled siRNA was formulated with DLinDAP, DLinDMA, DLinK-DMA, and DLinKC2-DMA labeled with spDiO and incubated with bmAPCs for the same time, at 10 μg/ml. Incubation was stopped in the same fashion after the same time intervals. Following treatment, bmAPCs were transferred into microcentrifuge tubes, spun at 12,000 rpm for 4 minutes and after three washes, they were resuspended in 300 μl FACS staining buffer. Samples were acquired using an LSRII flow cytometer to assess the presence of Cy5-labeled siRNA as well as spDiO-labeled LNPs intracellularly. The Cy5 fluorophore was excited using the HeNe 633 laser line and detected at the APC (FL 5) channel whereas the spDiO by the Argon laser and detected at FL1 channel. Data were acquired using FACSDiva software and analyzed by FlowJo software. Measurements were taken for 10,000 events. Fluorescence intensity was normalized against the untreated controls and was expressed as percent increase of mean fluorescence units.

Assessment of intracellular trafficking of LNP-siRNAs using ICM. To assess the intracellular distribution of encapsulated siRNA, a pulse-chase experiment was undertaken. BmMΦ and bmDCs were taken on day 8 of culture and grown on glass coverslips in 6-well plates until 70% confluent. Next, 2 μg/ml of Cy5-labeled siRNA free or encapsulated in DLinDAP, DLinDMA, DLinK-DMA, and DLinKC2-DMA LNPs was added and incubated for 2 hours. Incubation was stopped by removing the media and washing the coverslips twice with 4 °C PBS. Fresh media was then added and cells were placed at 37 °C for 1, 2, 4, and 8 hours to assess the siRNA

distribution over time. After each time point, cells were washed in cold PBS, fixed with 3% paraformaldehyde for 10 minutes, permeabilized with 0.1% saponin (Sigma, St Louis, MO), and stained with nuclear marker Propidium Iodide (Molecular Probes, Burlington, Canada) for 2 minutes to identify individual cells. After several washes, cover slips were then mounted onto microscope glass slides using slow fade medium (Molecular Probes) and examined under an immunofluorescent confocal microscope to assess the intracellular pattern of Cy5-labeled siRNA. Multiple images were captured with the ×60 objective following excitation with 633-nm laser line. ICM was also performed to visualize the presence of LNP-encapsulated Cy5-siRNA in endosomes and lysosomes over various incubation times. For this, after 0.5, 1, 2, 4, and 8 hours of siRNA chase and following fixation and permeabilization, cells were stained with rabbit anti-Early Endosomal Antigen 1 (EEA1, Sigma). After 16-hour incubation, another set of cell-containing glass slides were costained with EEA1 and goat anti-Lysosomal-Associated Membrane Protein 1 (LAMP1, Santa Cruz Biotechnology). Secondary Alexa-488-conjugated donkey anti-rabbit IgG (H+L) and donkey anti-goat IgG (H+L) Alexa-568 antibodies (Molecular Probes, OR, USA) were used to detect the endosomes and lysosomes, respectively. Isotype controls were used in all confocal microscopy experiments to confirm the specificity of antibody staining. All images were acquired using a Nikon-C1, TE2000-U immunofluorescent confocal microscope, and the EZ-C1 software. Fluorochromes were excited using the 488-nm, 568-nm, and 633-nm laser lines, and multiple images were captured using the ×60 objective.

Image quantification: For consistency, during the image analysis, the nuclei were shown in blue and the siRNA is shown in red. EZ-C1 3.20 FreeViewer software was used to quantify the intracellular presence and distribution of siRNA in primary bmAPCs. For this, multiple spots of interest were drawn within the cell areas of high fluorescence intensity corresponding to vesicular-like compartments and areas of low fluorescence corresponding to cell cytoplasm. The average fluorescence intensity was then obtained by subtracting the background, from the high and low intensity values of 5–10 cells in one microscopic field. A minimum of three images were examined for each treatment and time point. Data were normalized and expressed as mean (±SD) percent of punctate or diffuse pattern relative to total fluorescence intensity. Colocalization of two molecules was analyzed using ImageJ.1 to select single slices, and Adobe Photoshop 9.0 CS2 was used to merge images obtained from green, red, and blue channels. For consistency, endosomes, lysosomes, and the siRNA were shown in green, blue, and red, respectively. Colocalization of two different molecules was evaluated by the presence, intensity, and distribution of the yellow color (green + red) or purple (red + blue). For the quantification of colocalization following dual staining, a total of ~50 cells were examined. Absolute fluorescence intensity of green, red, blue and overlapping yellow and purple colors was obtained by multiplying the pixel value with the average intensity. The relative fluorescence intensity of all individual colors was then expressed as percent of total green (endosomes) or blue (lysosomes) fluorescence. Analysis was performed for each of the 20 Z slices acquired, providing an overall quantification of colocalization for the entire cell.

In vivo *gene silencing using DLinKC2-DMA LNPs.* All experiments involving mice were performed in accordance with the requirements of Canadian Council and UBC Committee on Animal Care. To study the *in vivo* gene silencing properties of DLinKC2-DMA-formulated siRNA, on day 0, 6- to 8-week-old C57Bl6 (Charles River) triplicate mice received by tail vein 5 mg/kg siRNA targeting *GAPDH* (si*GAPDH*), siRNA against Factor VII (siFVII) as control, formulated with DLinKC2-DMA LNPs, or PBS. They were euthanized 4 days later to assess the gene silencing capacity of si*GAPDH* in PerC and spleen-derived APCs. Peritoneal cavity APCs were obtained following peritoneal irrigation with 10 ml RPMI containing 5% FBS and centrifugation at 1,500 for 10 minutes. Spleens were harvested, minced in small pieces, and digested in 1 mg/ml collagenase D (Roche) and $CD11b^+$ and $CD11c^+$ cells were isolated *ex vivo* using magnetic beads as described previously.[50] Cell isolates were aliquoted, and *GAPDH* and α-Tubulin protein expression was assessed by flow cytometry as described. Data were acquired using LSRII flow cytometer after gating 10,000 events from the $F4\text{-}80^+/CD11b^+$ for MΦ or $CD11c^{high}$ for DCs and analyzed by FlowJo software. The other aliquot of spleen-derived APCs was span down, lysed, and protein expression was assessed by western blotting and quantified as described earlier.

Factor VII analysis, CD45 silencing assay and GFP Longevity of silencing. Both serum Factor VII silencing, *CD45* surface protein level measurements and 5′-RACE assay were done as described earlier.[11] GFP mice (n = 2) were injected i.v. with DLinKC2-DMA LNPs encapsulated GFP or Luc-specific siRNA at 3 mg/kg. Peritoneal cavity MΦ were collected after 3 days and GFP expression was analyzed by FACS on $CD11b^+$ cells. Remaining cells were plated in 96-well plate and GFP gene expression was analyzed by QPCR after 7, 14, and 21 days of post-injection.

***TNF-α determination* in vitro *and* in vivo.** Cytokine induction by MΦ treated with LNP-siRNA was also studied *in vitro* and *in vivo*. BmMΦ were aliquoted in 48-well plates and treated with 1 and 5 μg/ml siRNA encapsulated with LNPs under study. Control wells were treated with PBS or LPS 10 ng/ml. At 2 hours, Brefeldin A (Sigma) 10 μg/ml final was added to the wells, and plates were returned to incubator (37 °C) for further 15 hours. Next, cells were washed, fixed-permeabilized, and stained with CD11b-FITC to detect MΦ and anti-TNF-α PE antibody (Invitrogen) to quantify the presence of TNF-α intracellularly using flow cytometry. Mice were also injected with siRNA formulated with DLinKC2-DMA and 72 hours later; spleen MΦ were isolated, aliquoted, and stimulated with 5 ng/ml PMA and 1 μg/ml ionomycin (Sigma) for 5 hours followed by incubation with Brefeldin A at 2-hour incubation. Control wells treated with PBS or LPS were also included. After 15 hours at 37 °C, intracellular staining was performed as described to detect the TNF-α expression in MΦ using flow cytometry.

Statistical analysis. Student's *t*-test (paired, two-sample equal variance) was used to compare the siRNA efficacy following delivery with formulations under study as indicated. The difference was considered statistically significant when $P < 0.05$ (two-tailed distribution).

SUPPLEMENTARY MATERIAL

Figure S1. DLinDMA is more toxic to APCs than DLinDAP, DLinK-DMA and DLinKC2-DMA.

Figure S2. Loss of viable cells following treatment with LNPs is due to apoptosis.

Figure S3. Biodistribution of LNP-siRNA and intracellular delivery in tissue resident APCs, B and T-cells.

Figure S4. Animals treated with DLinKC2-DMA siRNA did not show weight loss.

Figure S5. Gene silencing in macrophages is RNAi mediated.

Figure S6. *In vivo* transfected DCs activate T-cells and migrate in lymph nodes.

Materials and Methods.

ACKNOWLEDGMENTS

The authors would like to acknowledge support from the Canadian Institutes for Health Research (CIHR) under UOP grant FRN 59836, as well as support from Tekmira Pharmaceuticals and Alnylam Pharmaceuticals. P.R.C. has a financial interest in Tekmira and receives grant support from Alnylam.

REFERENCES

1. Aagaard, L and Rossi, JJ (2007). RNAi therapeutics: principles, prospects and challenges. *Adv Drug Deliv Rev* **59**: 75–86.
2. Nabel, EG, Gordon, D, Yang, ZY, Xu, L, San, H, Plautz, GE *et al.* (1992). Gene transfer *in vivo* with DNA-liposome complexes: lack of autoimmunity and gonadal localization. *Hum Gene Ther* **3**: 649–656.
3. Liu, Y, Liggitt, D, Zhong, W, Tu, G, Gaensler, K and Debs, R (1995). Cationic liposome-mediated intravenous gene delivery. *J Biol Chem* **270**: 24864–24870.

4. Deshpande, D, Blezinger, P, Pillai, R, Duguid, J, Freimark, B and Rolland, A (1998). Target specific optimization of cationic lipid-based systems for pulmonary gene therapy. *Pharm Res* **15**: 1340–1347.
5. Wheeler, JJ, Palmer, L, Ossanlou, M, MacLachlan, I, Graham, RW, Zhang, YP *et al.* (1999). Stabilized plasmid-lipid particles: construction and characterization. *Gene Ther* **6**: 271–281.
6. Maurer, N, Wong, KF, Stark, H, Louie, L, McIntosh, D, Wong, T *et al.* (2001). Spontaneous entrapment of polynucleotides upon electrostatic interaction with ethanol-destabilized cationic liposomes. *Biophys J* **80**: 2310–2326.
7. Semple, SC, Klimuk, SK, Harasym, TO, Dos Santos, N, Ansell, SM, Wong, KF *et al.* (2001). Efficient encapsulation of antisense oligonucleotides in lipid vesicles using ionizable aminolipids: formation of novel small multilamellar vesicle structures. *Biochim Biophys Acta* **1510**: 152–166.
8. Morrissey, DV, Lockridge, JA, Shaw, L, Blanchard, K, Jensen, K, Breen, W *et al.* (2005). Potent and persistent *in vivo* anti-HBV activity of chemically modified siRNAs. *Nat Biotechnol* **23**: 1002–1007.
9. de Fougerolles, AR (2008). Delivery vehicles for small interfering RNA in vivo. *Hum Gene Ther* **19**: 125–132.
10. Whitehead, KA, Langer, R and Anderson, DG (2009). Knocking down barriers: advances in siRNA delivery. *Nat Rev Drug Discov* **8**: 129–138.
11. Akinc, A, Zumbuehl, A, Goldberg, M, Leshchiner, ES, Busini, V, Hossain, N *et al.* (2008). A combinatorial library of lipid-like materials for delivery of RNAi therapeutics. *Nat Biotechnol* **26**: 561–569.
12. Zimmermann, TS, Lee, AC, Akinc, A, Bramlage, B, Bumcrot, D, Fedoruk, MN *et al.* (2006). RNAi-mediated gene silencing in non-human primates. *Nature* **441**: 111–114.
13. Semple, SC, Akinc, A, Chen, J, Sandhu, AP, Mui, BL, Cho, CK *et al.* (2010). Rational design of cationic lipids for siRNA delivery. *Nat Biotechnol* **28**: 172–176.
14. Felgner, PL, Gadek, TR, Holm, M, Roman, R, Chan, HW, Wenz, M*et al.* (1987) Lipofection - a highly efficient, lipid-mediated dna-transfection procedure. *Proc Natl Acad Sci USA* **84**(21): 7413–7417.
15. Behr, JP, Demeneix, B, Loeffler, JP and Perez-Mutul, J (1989). Efficient gene transfer into mammalian primary endocrine cells with lipopolyamine-coated DNA. *Proc Natl Acad Sci USA* **86**: 6982–6986.
16. Ferrari, ME, Nguyen, CM, Zelphati, O, Tsai, Y and Felgner, PL (1998). Analytical methods for the characterization of cationic lipid-nucleic acid complexes. *Hum Gene Ther* **9**: 341–351.
17. Mislick, KA and Baldeschwieler, JD (1996). Evidence for the role of proteoglycans in cation-mediated gene transfer. *Proc Natl Acad Sci USA* **93**: 12349–12354.
18. Mounkes, LC, Zhong, W, Cipres-Palacin, G, Heath, TD and Debs, RJ (1998). Proteoglycans mediate cationic liposome-DNA complex-based gene delivery *in vitro* and in vivo. *J Biol Chem* **273**: 26164–26170.
19. Kopatz, I, Remy, JS and Behr, JP (2004). A model for non-viral gene delivery: through syndecan adhesion molecules and powered by actin. *J Gene Med* **6**: 769–776.
20. Hafez, IM, Ansell, S and Cullis, PR (2000). Tunable pH-sensitive liposomes composed of mixtures of cationic and anionic lipids. *Biophys J* **79**: 1438–1446.
21. Oja, CD, Semple, SC, Chonn, A and Cullis, PR (1996). Influence of dose on liposome clearance: critical role of blood proteins. *Biochim Biophys Acta* **1281**: 31–37.
22. Levchenko, TS, Rammohan, R, Lukyanov, AN, Whiteman, KR and Torchilin, VP (2002). Liposome clearance in mice: the effect of a separate and combined presence of surface charge and polymer coating. *Int J Pharm* **240**: 95–102.
23. Semple, SC, Harasym, TO, Clow, KA, Ansell, SM, Klimuk, SK and Hope, MJ (2005). Immunogenicity and rapid blood clearance of liposomes containing polyethylene glycol-lipid conjugates and nucleic Acid. *J Pharmacol Exp Ther* **312**: 1020–1026.
24. Parr, MJ, Bally, MB and Cullis, PR (1993). The presence of GM1 in liposomes with entrapped doxorubicin does not prevent RES blockade. *Biochim Biophys Acta* **1168**: 249–252.
25. Litzinger, DC, Brown, JM, Wala, I, Kaufman, SA, Van, GY, Farrell, CL *et al.* (1996). Fate of cationic liposomes and their complex with oligonucleotide in vivo. *Biochim Biophys Acta* **1281**: 139–149.
26. Kamps, JA, Morselt, HW and Scherphof, GL (1999). Uptake of liposomes containing phosphatidylserine by liver cells *in vivo* and by sinusoidal liver cells in primary culture: in vivo-in vitro differences. *Biochem Biophys Res Commun* **256**: 57–62.
27. Rothkopf, C, Fahr, A, Fricker, G, Scherphof, GL and Kamps, JA (2005). Uptake of phosphatidylserine-containing liposomes by liver sinusoidal endothelial cells in the serum-free perfused rat liver. *Biochim Biophys Acta* **1668**: 10–16.
28. Ichim, TE, Zhong, R and Min, WP (2003). Prevention of allograft rejection by *in vitro* generated tolerogenic dendritic cells. *Transpl Immunol* **11**: 295–306.
29. Hill, JA, Ichim, TE, Kusznieruk, KP, Li, M, Huang, X, Yan, X *et al.* (2003). Immune modulation by silencing IL-12 production in dendritic cells using small interfering RNA. *J Immunol* **171**: 691–696.
30. Gu, X, Xiang, J, Yao, Y and Chen, Z (2006). Effects of RNA interference on CD80 and CD86 expression in bone marrow-derived murine dendritic cells. *Scand J Immunol* **64**: 588–594.
31. Geisbert, TW, Hensley, LE, Kagan, E, Yu, EZ, Geisbert, JB, Daddario-DiCaprio, K *et al.* (2006). Postexposure protection of guinea pigs against a lethal Ebola virus challenge is conferred by RNA interference.*J Infect Dis* **193**(12): 1650–1657.
32. Soutschek, J, Akinc, A, Bramlage, B, Charisse, K, Constien, R, Donoghue, M *et al.* (2004). Therapeutic silencing of an endogenous gene by systemic administration of modified siRNAs. *Nature* **432**: 173–178.
33. Desjardins, M and Griffiths, G (2003). Phagocytosis: latex leads the way. *Curr Opin Cell Biol* **15**: 498–503.
34. Wisse, E, Jacobs, F, Topal, B, Frederik, P and De Geest, B (2008). The size of endothelial fenestrae in human liver sinusoids: implications for hepatocyte-directed gene transfer. *Gene Ther* **15**: 1193–1199.
35. Sanderson, S and Shastri, N (1994). LacZ inducible, antigen/MHC-specific T cell hybrids. *Int Immunol* **6**(3): 369–376.
36. Ghosh, YK, Visweswariah, SS and Bhattacharya, S (2000). Nature of linkage between the cationic headgroup and cholesteryl skeleton controls gene transfection efficiency. *FEBS Lett* **473**: 341–344.
37. McCaffrey, AP, Meuse, L, Pham, TT, Conklin, DS, Hannon, GJ and Kay, MA (2002). RNA interference in adult mice. *Nature* **418**: 38–39.
38. Lewis, DL, Hagstrom, JE, Loomis, AG, Wolff, JA and Herweijer, H (2002). Efficient delivery of siRNA for inhibition of gene expression in postnatal mice. *Nat Genet* **32**: 107–108.
39. Zender, L, Hutker, S, Liedtke, C, Tillmann, HL, Zender, S, Mundt, B *et al.* (2003). Caspase 8 small interfering RNA prevents acute liver failure in mice. *Proc Natl Acad Sci USA* **100**: 7797–7802.
40. Aouadi, M, Tesz, GJ, Nicoloro, SM, Wang, M, Chouinard, M, Soto, E *et al.* (2009). Orally delivered siRNA targeting macrophage Map4k4 suppresses systemic inflammation. *Nature* **458**: 1180–1184.
41. Peer, D, Park, EJ, Morishita, Y, Carman, CV and Shimaoka, M (2008). Systemic leukocyte-directed siRNA delivery revealing cyclin D1 as an anti-inflammatory target. *Science* **319**: 627–630.
42. Zheng, X, Vladau, C, Zhang, X, Suzuki, M, Ichim, TE, Zhang, ZX *et al.* (2009). A novel *in vivo* siRNA delivery system specifically targeting dendritic cells and silencing CD40 genes for immunomodulation. *Blood* **113**: 2646–2654.
43. Vial, T, Choquet-Kastylevsky, G and Descotes, J (2002). Adverse effects of immunotherapeutics involving the immune system. *Toxicology* **174**: 3–11.
44. Descotes, J (2009). Immunotoxicity of monoclonal antibodies. *MAbs* **1**: 104–111.
45. Akinc, A, Querbes, W, De, S, Qin, J, Frank-Kamenetsky, M, Jayaprakash, KN *et al.* (2010). Targeted delivery of RNAi therapeutics with endogenous and exogenous ligand-based mechanisms. *Mol Ther* **18**: 1357–1364.
46. Lazarovits, AI, Poppema, S, Zhang, Z, Khandaker, M, Le Feuvre, CE, Singhal, SK *et al.* (1996). Prevention and reversal of renal allograft rejection by antibody against CD45RB. *Nature* **380**: 717–720.
47. Tan, J, Town, T, Mori, T, Wu, Y, Saxe, M, Crawford, F *et al.* (2000). CD45 opposes beta-amyloid peptide-induced microglial activation via inhibition of p44/42 mitogen-activated protein kinase. *J Neurosci* **20**: 7587–7594.
48. Basadonna, GP, Auersvald, L, Khuong, CQ, Zheng, XX, Kashio, N, Zekzer, D *et al.* (1998). Antibody-mediated targeting of CD45 isoforms: a novel immunotherapeutic strategy. *Proc Natl Acad Sci USA* **95**: 3821–3826.
49. Kortylewski, M, Swiderski, P, Herrmann, A, Wang, L, Kowolik, C, Kujawski, M *et al.* (2009). *In vivo* delivery of siRNA to immune cells by conjugation to a TLR9 agonist enhances antitumor immune responses. *Nat Biotechnol* **27**: 925–932.
50. de Jong, SD, Basha, G, Wilson, KD, Kazem, M, Cullis, P, Jefferies, W *et al.* (2010). The immunostimulatory activity of unmethylated and methylated CpG oligodeoxynucleotide is dependent on their ability to colocalize with TLR9 in late endosomes. *J Immunol* **184**: 6092–6102.